Toward More Efficient CCSD(T) Calculations of Intermolecular Interactions in Model Hydrogen-Bonded and Stacked Dimers

Pavlína Dedíková,[†,‡] Michal Pitoňák,[§] Pavel Neogrády,[†] Ivan Černušák,[†] and Miroslav Urban*[,†]

Department of Physical and Theoretical Chemistry, Faculty of Natural Sciences, Comenius University, Mlynská dolina, SK-842 15 Bratislava, Slovakia, and Institute of Organic Chemistry and Biochemistry, Academy of Sciences of the Czech Republic, Flemingovo nám. 2, CZ-16610 Prague, Czech Republic

Received: April 18, 2008; Revised Manuscript Received: June 11, 2008

Interaction energies of the model H-bonded complexes, the formamide and formamidine dimers, as well as the stacked formaldehyde and ethylene dimers are calculated by the coupled cluster CCSD(T) method. These systems serve as a model for H-bonded and stacking interactions, typical in molecules participating in biological systems. We use the optimized virtual orbital space (OVOS) technique, by which the dimension of the space of virtual orbitals in coupled cluster CCSD(T) calculations can be significantly reduced. We demonstrate that when the space of virtual orbitals is reduced to 50% of the full space, which means reducing computational demands by 1 order of magnitude, the interaction energies for both H-bonded and stacked dimers are affected by no more than 0.1 kcal/mol. This error is much smaller than the error when interaction energies are calculated using limited basis sets.

1. Introduction

Accurate data of interaction energies of different hydrogen-bonded (H-bonded) structures as well as stacking interactions are essential for understanding the key aspects of forces contributing to the stabilization of biomolecules and particularly DNA. Because experimental interaction energies of individual molecules important in biological systems are mostly not available, theoretical methods may serve as a useful source of information in this area. The physical background behind H-bonded systems and stacking interactions is different. The former is governed by a complicated interplay of electrostatic energy, charge transfer, exchange repulsion, and some contribution from the London dispersion interaction, in stacking systems dominated by dispersion forces primarily due to (aromatic) $\pi-\pi$ interactions. While H-bonded systems can be described by density functional theory techniques relatively accurately, these methods have notorious problems in describing dispersion interactions, even if in this area one can notice significant progress in recent past few years.[1,2] However, for a proper description of the relative importance of all forces contributing to the stability of bonding blocks in biological systems,[3] it is essential that all interactions are described with a similar accuracy. This concerns also solvent effects. A complication arises from the fact that real biologically important molecules are large, even if we restrict ourselves to isolated molecules and forget for a while the environment in which all biological processes occur. Therefore, it is crucial to describe various components participating in interactions in biological systems with a similar accuracy for quite large molecules. The same holds in other areas where interaction energies play an important role.

A "golden standard" for accurate calculations of molecular properties and molecular interactions is presently the coupled cluster CCSD(T) method[4] with the iterative treatment of the single and double excitation amplitudes, which are subsequently used for perturbative calculations of triples.[5,6] This method is applicable for closed-shell and high-spin open-shell systems in a straightforward way. Unfortunately, computational demands are the most time-consuming steps in the CCSD(T) scale with the number of orbitals as $N_o^3N_v^3/N_o^2N_v^4$ and $N_o^3N_v^4$ (in triples), where N_o and N_v are the number of occupied and virtual orbitals, respectively. Therefore, calculations for larger molecules suitable for representing realistic systems in various chemical, physical, or biological applications become rapidly prohibitively expensive. Most robust CCSD(T) programs[7,8] employing extensive parallelism, Cholesky decomposition, or some other techniques are constructed for calculations with, say, 100 explicitly correlated electrons employing basis sets as large as 1500−2000 contracted Gaussian basis set functions. This is really a challenge because such calculations require enormous computer time and very good computational facilities. One way for relieving extreme computer demands, namely, employing the OVOS technique, was recently proposed in our group, many years after the first attempts in this direction were made by Bartlett, Adamowicz and Sadlej.[9,10] More recently, we have introduced an alternative way for obtaining OVOS,[11] which proved to be very successful in applications to reaction energies, vibrational frequencies,[11] and electric properties as dipole moments and dipole polarizabilities[11,12] as well as in relativistic calculations.[13] A comprehensive review of the performance of the method was summarized in ref 14. A considerable step forward in employing new techniques in CCSD(T) calculations was made recently in calculations of truly large systems like H-bonded and stacked structures of the uracil dimer.[15]

The purpose of this paper is to show that the OVOS technique is useful also in calculations of H-bonded systems and in molecules bonded primarily by dispersion forces, as is the case in stacked systems. Therefore, we have calculated four model systems representing H-bonded and stacking interactions. All of them are typical structural units resembling interactions present in the DNA structure. H-bonding is represented by the

* To whom correspondence should be addressed. E-mail: urban@fns.uniba.sk.
† Comenius University.
‡ E-mail: dedikova@fns.uniba.sk.
§ Academy of Sciences of the Czech Republic.

10.1021/jp8033903 CCC: $40.75
Published on Web 07/02/2008

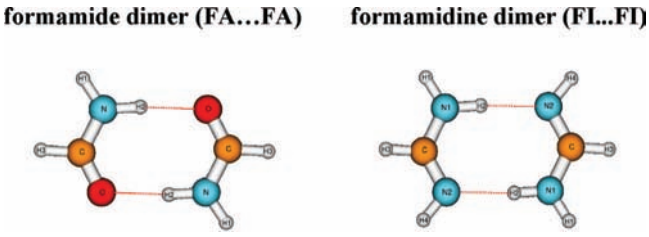

Figure 1. C_{2h} geometries of the model H-bonded complexes, the formamide dimer (FA···FA) and the formamidine dimer (FI···FI), optimized at the MP2/6-31G** level. Bond lengths are in angstroms and angles in degrees. FA···FA: r(C═O) = 1.234, r(C−N) = 1.349, r(C−H) = 1.114, r(N−H1) = 1.001, r(N−H2) = 1.031, r(0···H) = 1.858, α(OCN) = 125.8, α(NCH3) = 113.2, α(CNH1) = 119.4. FI···FI: r(C−N1) = 1.349, r(C−N2) = 1.295, r(N2−H4) = 1.015, r(C−H3) = 1.093, r(N1−H2) = 1.025, r(N1−H1) = 1.002, r(N···H) = 1.944, α(N1CN2) = 122.9, α(H4N2C) = 109.4, α(CN1H1) = 119.5, α(N1CH3) = 113.8, α(CN1H2) = 120.9.

Figure 2. Geometries of model stacked complexes. C_{2h} structure of the formaldehyde dimer (FO···FO) and D_{2h} structure of the ethylene dimer (ET···ET). Monomers were optimized using the MP2/6-31G** method. Bond lengths are in angstroms and angles in degrees. Monomers in both dimers are separated by 3.3 Å. FO···FO: r(C═O) = 1.2202, r(C−H) = 1.1002, α(HCH) = 115.5, α(HCO) = 122.25. ET···ET: r(C═C) = 1.335, r(C−H) = 1.0807, α(HCH) = 116.8, α(HCC) = 121.6.

formamide dimer (FA···FA) and the formamidine dimer (FI···FI) (Figure 1). Both dimers are planar and have two N−H···N or N−H···O hydrogen bonds in their C_{2h} cyclic structures taken from Pittner and Hobza.[16] These structures were previously studied theoretically and experimentally by many authors (formamide dimer[17–23] and formamidine dimer[22,24]). The formaldehyde dimer (FO···FO) and the ethylene dimer (ET···ET) represent stacking interactions (Figure 2). In the FO···FO complex, the orientation of dipole moments is antiparallel, leading to an attractive component of the lowest-order electrostatic interaction. The formaldehyde dimer exhibits C_{2h} symmetry. The initial geometry of the ethylene dimer is represented by parallel ethylene molecules with no parallel displacement of both subsystems (the "sandwich" complex; D_{2h} symmetry). These geometries of ET···ET and FO···FO dimers do not represent equilibrium geometries but serve only as models of stacked structures. In subsequent calculations, we have verified the performance of the OVOS technique also for parallel-displaced ethylene dimer geometries. There are only a few studies of this antiparallel formaldehyde structure[25–27] and the D_{2h} ethylene structure.[28,29] The lowest-energy conformations were experimentally and theoretically determined to be the ethylene D_{2d} dimer[30,31] and the formaldehyde C_s dimer.[27,32,33] All studied H-bonded and stacked systems were previously calculated by Pittner and Hobza.[16]

2. Calculations

Geometries of H-bonded systems considered in this study were optimized at the MP2/6-31G** level of theory by Pittner and Hobza.[16] All CCSD(T) calculations were carried out by the MOLCAS[34] quantum-chemical package, in which our CC programs and the OVOS module[35] were implemented. The following Dunning's correlation consistent basis sets were used: cc-pVXZ (X = D, T, Q) and aug-cc-pVXZ (X = D, T, Q, 5).[36,37] Corrections for the basis set superposition error (BSSE) were calculated via the counterpoise (CP) correction scheme.[38] The structures of monomers in both stacked complexes were obtained at the MP2/6-31G** level of theory using the *Gaussian03*[39] program package. The planes of the subsystems in both model stacked dimers were separated by 3.3 Å. Such a distance is typical for stacked DNA base pairs. The sandwich D_{2h} structure of the ethylene dimer represents a transition state connecting the two minima corresponding to parallel-displaced structures. The "sandwich" D_{2h} structure of the FO···FO dimer with no displacement of the two formaldehyde planes is a minimum. This was verified at a fixed distance (R = 3.3 Å) between two planes at the CCSD(T)/aug-cc-pVTZ level. The optimum geometry represents the two formaldehyde molecules with antiparallel molecular planes having C and O atoms located in the rectangular arrangement (Figure 2).

2a. Synopsis of the OVOS Method. The essence of the OVOS approach[11,14] lies in reducing computational demands in CC calculations by truncating the dimension of the virtual orbital space (VOS) without a significant loss of accuracy. Our implementation of the OVOS approach is based on the requirement that the overlap of the first-order wave function defined in the reduced OVOS space and the first-order wave function in the full VOS, respectively, is maximal:

$$L = \langle \phi_0 | \tau_{\mathrm{MP2}} | \tau_{\mathrm{MP2}}^{\mathrm{OVOS}} | \phi_0 \rangle \tag{1}$$

In the overlap functional L (eq 1), only double-excitation amplitudes are needed for closed-shell systems. Within OVOS, the $\tau_{\mathrm{MP2}}^{\mathrm{OVOS}}$ (the shorter notation is τ_2^{OVOS}) operator is defined as

$$\tau_2^{\mathrm{OVOS}} = \frac{1}{4} \sum_{i,j,a^*,b^*} t_{ij}^{a^*b^*} a^{*\dagger} i b^{*\dagger} j \tag{2}$$

($t_{ij}^{a^*b^*}$ are the double-excitation amplitudes accompanied by their respective creation and annihilation operators; indices with asterisks correspond to the virtual orbitals in the OVOS space.) Excitation operators in the full space are defined analogously.

The interaction energy ΔE is defined as a difference between the total energy of the supersystem and the sum of energies of both subsystems. The correlation energies of all species were evaluated by the second-order (MP2)[40] and CCSD(T)[4] methods. When calculating CCSD(T) energies by using the OVOS approach, we can directly use energies (denoted as CCSD(T)$^{\mathrm{OVOS}}$ energies) resulting from the truncated OVOS. The scope of the OVOS truncation is measured as a percentage of the number of virtual orbitals considered in the optimized virtual space with respect to the full VOS. Even more accurate results are obtained when we exploit the MP2 energy calculated in the full VOS (needed anyway in the optimization procedure, eq 1) for correcting the CCSD(T)$^{\mathrm{OVOS}}$ energy by the difference X_2.[11,14] So-corrected OVOS CCSD(T) energies are denoted as CCSD(T)$_{\mathrm{MP2}}^{\mathrm{OVOS}}$ or, in short, CCSD(T)$_2^{\mathrm{OVOS}}$. Utilizing CCSD(T)$_2^{\mathrm{OVOS}}$ energies of the supersystem and the subsystems, we calculate the interaction energy including the X_2 correction as

$$\Delta E_{\mathrm{CCSD(T)}_2}^{\mathrm{OVOS}} = \Delta E_{\mathrm{MP2}}^{\mathrm{fullVOS}} + X_2 \tag{3}$$

with

$$X_2 = \Delta E_{\mathrm{CCSD(T)}}^{\mathrm{OVOS}} - \Delta E_{\mathrm{MP2}}^{\mathrm{OVOS}} \tag{4}$$

In X_2 we use the difference between the CCSD(T)$^{\mathrm{OVOS}}$ and MP2$^{\mathrm{OVOS}}$ energies, both calculated in the truncated OVOS space. The procedure, which utilizes the full VOS at the MP2 level

TABLE 1: SCF, MP2, and CCSD(T) Interaction Energies of a H-Bonded Formamide Dimer (FA···FA; Figure 1) with the Full VOS (100%) and OVOS Reduced to 80, 70, 60, and 50%[a]

			CCSD(T)	$CCSD(T)_2^{OVOS}$			
basis set	SCF	MP2	100%	80%	70%	60%	50%
cc-pVDZ	−12.01	−12.00	−11.97	−12.29	−12.32	−12.43	−12.43
cc-pVTZ	−12.40	−14.50	−14.61	−14.58	−14.54	−14.61	−14.50
cc-pVQZ	−12.56	−15.43	−15.68		−15.68	−15.68	−15.65
aug-cc-pVDZ	−12.43	−14.25	−14.33	−14.32	−14.31	−14.30	−14.38
aug-cc-pVTZ	−12.47	−15.28	−15.55	−15.55	−15.55	−15.47	−15.46
aug-cc-pVQZ	−12.56	−15.73	−16.05			−16.03	
aug-cc-pV5Z	−12.56	−15.87				−16.18	
QZ → 5Z [b]						−16.34	
aug-cc-pVDZ [c]	−12.66	−14.33	−14.44				

[a] BSSE-corrected[38] interaction energies in kcal/mol. 1s orbitals of C, O, and N are frozen. [b] CCSD(T) CBS extrapolation (aug-cc-pVQZ → aug-cc-pV5Z). [c] Reference 16.

(eq 3) and uses the X_2 correction, which requires demanding CCSD(T) calculation only in the truncated OVOS space (eq 4), resembles the approach advocated by Jurecka and Hobza.[21] They have shown that the difference between the CCSD(T) and MP2 interaction energies [CCSD(T) − MP2] has a small basis set dependence. The true stabilization energy ΔE is then computed as a sum of the MP2 interaction energy with a larger basis set and a correction term obtained using a smaller basis set:

$$\Delta E = \Delta E_{\text{extended}}^{\text{MP2}} + \lfloor \Delta E_{\text{small}}^{\text{CCSD(T)}} - \Delta E_{\text{small}}^{\text{MP2}} \rfloor \qquad (5)$$

The applicability of this approach is based on the assumption that the difference between the CCSD(T) and MP2 energies depends on the basis set only little. This is not always true, however.

One important note concerns the BSSE, which must be eliminated in supermolecule calculations of interaction energies with finite unsaturated basis sets. The standard Boys and Bernardi CP correction[38] was applied in calculations employing full VOS. However, in calculations using truncated OVOS, the standard approach must be modified. Let us remind everyone that the supersystem and both BSSE-corrected subsystems are calculated with the same atomic orbital (AO) basis set. Obviously, the supersystem and the subsystems have different numbers of occupied orbitals, so that the dimension of the full VOS is also different even if the AO basis set is the same. Truncating OVOS by, say, 50% in both the supersystem and the subsystem, respectively, then also leads to different numbers of virtual orbitals for both species. However, the optimization efficiency in maximizing the functional L (eq 1) depends on the dimension of the starting full VOS.[12,13,35] Well-balanced dimension of the truncated OVOS for all participating systems is essential for highly accurate results. This means that we need to adjust the dimension of the truncated OVOS in order to account for the different dimensions of the space of occupied/virtual orbitals for the supersystem and all subsystems. Our computational experience (especially in noncovalent systems) shows that for a given truncation of OVOS the condition of the "balanced" truncation leads to approximately the same ratio between the number of occupied and the number of truncated optimized virtual orbitals for the supersystem and the subsystems. The deviation of this ratio from a constant value strongly correlates with the extent to which the orbital picture is changed going from the supersystem to the subsystems.

Our strategy for "balancing" the optimization efficiency is based on the calculation of the percentage of the value of the optimization functional L recovered in the truncated OVOS compared to its value in the full VOS (which represents 100%). According to our experience, the best possible mutual agreement of the percentage of the optimization functional with respect to full VOS for all involved species leads to well-balanced results for BSSE-corrected interaction energies. In fact, this requirement is also useful in truncated OVOS calculations of other processes in which the orbital framework is changed, like in reaction energies, calculations of the ionization potential, electron affinities, etc.[11–14,41,42]

The methodology used in this paper follows the arguments described above. First, we select a dimension of the truncated OVOS in all irreducible symmetry representations of the supersystem. This dimension is expressed in percentage with respect to the full VOS (dimension of the full VOS represents 100%). For so-selected truncated OVOS, we obtain the percentage of the optimization functional with respect to its value in the full VOS. Then we proceed in searching for a proper truncation of OVOS for subsystems starting with a reasonable estimate of the dimension of OVOS and "tune" the truncation of OVOS until it reproduces the percentage of the optimization functional obtained previously for the supersystem. One interesting consequence of this procedure is that computational demands for calculations of the BSSE-corrected CCSD(T) energies of the subsystems are approximately the same as those for the calculations of plain, BSSE-uncorrected subsystem energies. This follows from our finding that, as a rule, the dimension of the truncated OVOS for the subsystem with the supersystem basis set is almost the same as that when we use only AO basis functions for a particular subsystem.

3. Results and Discussion

3a. H-Bonded Dimers. Full VOS and differently truncated OVOS CCSD(T) interaction energies along with self-consistent-field (SCF) and MP2 results for H-bonded dimers (FA···FA and FI···FI) are summarized in Tables 1 and 2. The truncated dimension of virtual orbitals used in OVOS is expressed approximately in percentage with respect to the full VOS for any specific basis set. Our SCF, MP2, and the full space CCSD(T) interaction energies for the FI···FI dimer agree completely with the numbers published by Pittner and Hobza.[16] The small difference between our interaction energies and the values in ref 16 for the FA···FA dimer is caused by slight numerical inaccuracies of the geometry parameters.

It is clear from Tables 1 and 2 that the SCF component of the interaction energy for both H-bonded dimers is rather insensitive to the basis set quality. As expected, the electron correlation contribution varies with the basis set significantly. The CCSD(T) correlation contribution for the FA···FA dimer increases from 0% of the total ΔE interaction energy with cc-

TABLE 2: SCF, MP2, and CCSD(T) Interaction Energies of a H-Bonded Formamidine Dimer (FI···FI; Figure 1) with the Full VOS (100%) and OVOS Reduced to 80, 70, 60, and 50%[a]

			CCSD(T)	$CCSD(T)_2^{OVOS}$			
basis set	SCF	MP2	100%	80%	70%	60%	50%
cc-pVDZ	−10.73	−13.08	−12.39	−12.60	−12.67	−12.27	−12.79
cc-pVTZ	−10.67	−14.84	−14.41	−14.41	−14.39	−14.36	−14.17
cc-pVQZ	−10.71	−15.57	−15.23			−15.23	
aug-cc-pVDZ	−10.49	−14.40	−13.84	−13.82	−13.81	−13.77	−13.80
aug-cc-pVTZ	−10.70	−15.52	−15.20	−15.20	−15.22	−15.22	−15.29
aug-cc-pVQZ	−10.73	−15.73				−15.60	
TZ → QZ [b]						−15.88	
aug-cc-pVDZ [c]	−10.49	−14.41	−13.84				

[a] BSSE-corrected[38] interaction energies in kcal/mol. 1s orbitals of C and N are frozen. [b] CCSD(T) CBS extrapolation (aug-cc-pVTZ → aug-cc-pVQZ). [c] Reference 16.

pVDZ up to 22% with the aug-cc-pVQZ basis set. In the case of the FI···FI pair, the electron correlation contribution increased from 13% of the total ΔE with the small cc-pVDZ basis set to 30% with the larger aug-cc-pVTZ basis set. The final $\Delta E_{CCSD(T)}$ interaction energies with these two basis sets differ by as much as 4.1 kcal/mol for FA···FA and by 2.8 kcal/mol for the FI···FI H-bonded dimers.

Total interaction energies of both H-bonded dimers are represented by MP2 quite satisfactorily. We note, however, that the difference between the MP2 and CCSD(T) interaction energy is basis set dependent. It varies from −0.03 to +0.32 kcal/mol for FA···FA and from −0.69 to −0.32 kcal/mol for FI···FI with cc-pVXZ and aug-cc-pVXZ basis sets. Clearly, techniques relying on the constant difference between MP2 and CCSD(T) interaction energies work only with larger basis sets, at least aug-cc-pVTZ. Using the full VOS CCSD(T) data, the $\Delta E_{CCSD(T)}$ interaction energy obtained with aug-cc-pVTZ and aug-cc-pVQZ basis sets is by 0.3 kcal/mol higher than the ΔE_{MP2} interaction energy for the FA···FA dimer. The trend for the FI···FI dimer is opposite. This dimer is by about 0.3 kcal/mol less stable at the CCSD(T) level than at the MP2 level. For selected geometries and with large aug-cc-pVTZ and aug-cc-pVQZ basis sets, the MP2 hydrogen binding energy in FI···FI is slightly higher or the same as that in the FA···FA dimer. Different relative stabilities are calculated at the CCSD(T) level: The hydrogen bond in FA···FA is stronger by about 0.3−0.4 kcal/mol than it is in FI···FI. According to data in Tables 1 and 2, it is gratifying that the basis set dependence and tiny differences in relative $CCSD(T)_2^{OVOS}$ binding energies for the two representative H-bonded systems are very well reproduced with OVOS truncated to about 60% or even 50% of the full VOS. Differences between the H-bond strength with the full and with the truncated OVOS space for the aug-cc-pVXZ series are smaller than 0.1 kcal/mol, typically about 0.05 kcal/mol. The smallest errors (0.02 kcal/mol) for interaction energies are obtained with aug-cc-pVQZ (for FA···FA) and aug-cc-pVTZ (for FI···FI) basis sets with OVOS truncated to 60% of the full VOS. OVOS calculations with the cc-pVXZ series exhibit larger errors, particularly for the smallest cc-pVDZ basis set. Deviations of interaction energies with OVOS truncated to 50% from $\Delta E_{CCSD(T)}$ with the full VOS of the smallest cc-pVDZ basis set are about 0.5 kcal/mol for FA···FA and 0.4 kcal/mol for the FI···FI, respectively. Such errors still represent less than 4% of the total ΔE obtained in the full space. Nevertheless, this basis set is not recommended for calculating H-bonding interactions anyway because $\Delta E_{CCSD(T)}$ interaction energies with this basis set differ from the results with more extended bases by as much as 3−4 kcal/mol, irrespective of the virtual space; it does not matter much whether we use the full or the truncated

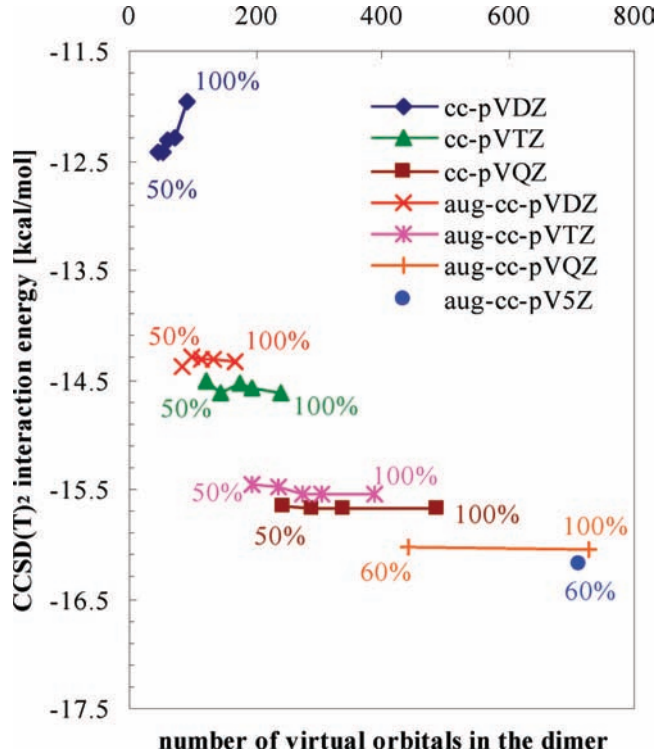

Figure 3. CCSD(T) interaction energies of the formamide dimer (FA···FA; Figure 1) using cc-pVXZ (X = D, T, Q) and aug-cc-pVXZ (X = D, T, Q, 5) basis sets. 1s orbitals of C, N, and O are frozen. Full VOS (100%) CCSD(T) and $CCSD(T)_2^{OVOS}$ interaction energies with OVOS truncated to 80−50%, respectively, are plotted as a function of the number of employed dimer virtual orbitals.

OVOS virtual space. Using the results with the cc-pVDZ basis set in extrapolations to the complete basis set (CBS) limit is not recommended as well.

The interplay between the basis set dependence of the interaction energy for the FA···FA and FI···FI H-bonded dimers and the performance of the OVOS technique is demonstrated in Figures 3 and 4, respectively, with the cc-pVXZ (X = D, T, Q) and aug-cc-pVXZ (X = D, T, Q, 5) basis set series. In these figures, we plot the dependence of the $CCSD(T)_2$ interaction energy on the number of virtual orbitals considered in the CCSD(T) calculation with the full VOS and with OVOS truncated to 80, 70, 60, and 50%, respectively. Very transparent is the relatively large dependence of $\Delta E_{CCSD(T)}$ on the size and quality of the basis set. The main message conveyed by these figures is the observation that significantly more accurate CCSD(T) interaction energies (and, frequently, for the lower price) are obtained with larger basis sets with OVOS truncated

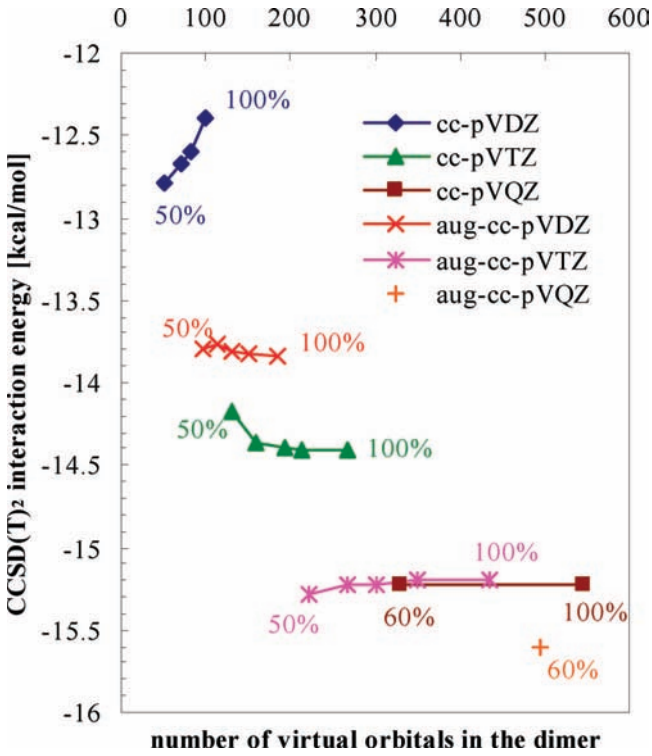

Figure 4. CCSD(T) interaction energies of the formamidine dimer (FI···FI; Figure 1) using cc-pVXZ (X = D, T, Q) and aug-cc-pVXZ (X = D, T, Q) basis sets. 1s orbitals of C and N are frozen. Full VOS (100%) CCSD(T) and CCSD(T)$_2^{OVOS}$ interaction energies with OVOS truncated to 80−50%, respectively, are plotted as a function of the number of employed dimer virtual orbitals.

to 60% or even 50% of the full space than with the full VOS of a smaller basis set. Both H-bonded systems studied in this work exhibit similar patterns of the basis set effects, which holds for the full VOS and for truncated OVOS. We wish to stress that with larger basis sets results with OVOS truncated down to 50% are very stable. Smaller basis sets having less virtual orbitals are more sensitive to the extent to which OVOS is truncated.

Figures 3 and 4 clearly demonstrate that errors introduced by truncating OVOS are much smaller than the basis set effects. We can demonstrate this assertion by a simple comparison. In the case of the FA···FA complex calculated with the aug-cc-pVTZ basis set and OVOS truncated to 50%, we obtain $\Delta E^{OVOS}_{CCSD(T)_2}$, which is more than 1.13 kcal/mol higher (and closer to the CBS limit) than the CCSD(T) interaction energy with the full VOS with a smaller aug-cc-pVDZ basis set. Analogously, $\Delta E^{OVOS}_{CCSD(T)_2}$ calculated with the cc-pVQZ basis set and OVOS truncated to 50% (243 virtuals) is by 1.04 kcal/mol higher (and closer to more demanding calculations) than $\Delta E_{CCSD(T)}$ using full VOS of a smaller cc-pVTZ basis set (240 virtuals). Both calculations require similar computer time. Analogous conclusions are also valid for the FI···FI dimer. When comparing computer demands, we should realize that by using the virtual space reduced by OVOS to about 50% of the full VOS, about 90% of the computer time is saved without any significant loss of accuracy.

Concerning computer time with the OVOS technique, a typical example is the CCSD(T) calculation of the formamide dimer with the aug-cc-pVQZ basis set (753 contracted Gaussians). The dimer has 48 electrons, of which 36 were correlated in CCSD(T). Full VOS contains 729 virtuals; the total computer time for CCSD(T) was 13 328 min using our workstation (two nodes, dual AMD Opteron Processor 250, 2.4 GHz, RAM 8GB, scratch disk capacity 500GB). With OVOS truncated to 60% (441 virtuals), the total computer time dropped to 2370 min. The saving factor in CCSD(T) is 5.6; the theoretical saving factor for the most demanding step is 7.7. With OVOS truncated to 50%, the calculation usually needs 10% of the full VOS time. In the largest calculation for the FA···FA dimer presented in this work, we used the aug-cc-pV5Z basis set. The total number of contracted Gaussians is 1242. Considering such a large basis set in CCSD(T) using full VOS (1218 virtual orbitals) is quite demanding with a standard workstation. Employing our efficient parallel CCSD(T) code with OVOS reduced to about 60%, with 711 virtuals, makes the CCSD calculation relatively easy. When more than 40 electrons are correlated, calculations of triples in CCSD(T) become dominant.

TABLE 3: SCF, MP2, and CCSD(T) Interaction Energies of a H-Bonded Formamide Dimer with the Full VOS (100%) and OVOS Reduced to 60% Including a Geometry-Dependent Approach

		CCSD(T)	CCSD(T)$_2^{OVOS}$
basis set	MP2	100%	60%
aug-cc-pVDZ	−13.54	−13.69	−13.66
aug-cc-pVTZ	−13.81	−14.09	−14.01
aug-cc-pVQZ	−14.11	−14.43	−14.42
E_{CBS}(T→Q) [a]	−14.33	−14.68	−14.72
aug-cc-pVDZ[b]	−13.39		
aug-cc-pVTZ[b]	−14.11		
aug-cc-pVQZ[b]	−14.48		
E_{CBS}(D→Q) [b]		−14.80	

[a] CCSD(T) CBS extrapolation (aug-cc-pVTZ → aug-cc-pVQZ). [b] Frey and Leutwyler.[18]

The basis set convergence of ΔE for the formamide dimer is relatively slow at the correlated level (for details, see Table 1). The full VOS CCSD(T) interaction energy with the aug-cc-pVQZ basis set (16.05 kcal/mol) differs from aug-cc-pVTZ by 0.50 kcal/mol. Further extension of the basis set to aug-cc-pV5Z is practical only with OVOS truncated to 60%. So-calculated ΔE is 16.18 kcal/mol, which is 0.15 kcal/mol lower than ΔE with the aug-cc-pVQZ basis set. This is an almost converged result. Because OVOS results with large basis sets differ typically from the full VOS results to within 0.01−0.02 kcal/mol, our final ΔE should be considered as highly reliable. Similar behavior is also valid for the formamidine dimer.

3b. Geometry-Relaxed Calculations of the Interaction Energy. Subsystems in H-bonded compounds frequently undergo substantial geometry relaxation due to the interaction. Such geometry relaxation was taken into account for example in calculations of the FA···FA dimer by Frey a Leutwyler.[18] When correcting ΔE for BSSE additional energies of the subsystems must be calculated using the supersystem basis set. Standard expression for the BSSE corrected interaction energy is

$$\Delta E = E^{AB}_{AB} - E^{AB}_{A} - E^{AB}_{B} \quad (6)$$

with E^{AB}_{AB}, E^{AB}_{A}, and E^{AB}_{AB} being energies of the supersystem and the subsystems A and B, respectively, calculated in the same, i.e., the supersystem, basis set. When the interaction energy is weak, it is common that subsystems are considered in their "frozen" geometries corresponding to the separated species; i.e., we calculate energies $E^{AB}_{A}(R_A)$ and $E^{AB}_{B}(R_B)$. When considering the geometry deformation of the subsystems occurring in the supersystem, the "geometry-dependent approach" can be used,[43,44]

TABLE 4: SCF, MP2, and CCSD(T) Interaction Energies of a Stacked Formaldehyde Dimer (FO···FO; Figure 2) with the Full VOS (100%) and OVOS Reduced to 80, 70, 60, and 50%[a]

			CCSD(T)	$CCSD(T)_2^{OVOS}$			
basis set	SCF	MP2	100%	80%	70%	60%	50%
cc-pVDZ	−1.69	−1.09	−1.21	−1.26	−1.29	−1.29	−1.28
cc-pVTZ	−2.01	−1.86	−1.91	−1.93	−1.92	−1.90	−1.89
cc-pVQZ	−2.10	−2.22	−2.27	−2,29	−2.28	−2.27	−2.28
aug-cc-pVDZ	−2.18	−2.21	−2.26	−2.27	−2.26	−2.25	−2.25
aug-cc-pVTZ	−2.14	−2.37	−2.43	−2.42	−2.43	−2.42	−2.41
aug-cc-pVQZ	−2.14	−2.46	−2.51	−2.51	−2.51	−2.49	−2.49
aug-cc-pV5Z	−2.14	−2.49				−2.53	
QZ → 5Z [b]						−2.57	
aug-cc-pVDZ [c]	−2.08	−2.13	−2.18				

[a] BSSE-corrected[38] interaction energies in kcal/mol. 1s orbitals of C and O are frozen. [b] CCSD(T) CBS extrapolation (aug-cc-pVQZ → aug-cc-pV5Z). [c] Pittner and Hobza.[16]

TABLE 5: SCF, MP2, and CCSD(T) Interaction Energies of a Stacked Ethylene Dimer (ET···ET; Figure 2) with the Full VOS (100%) and OVOS Reduced to 80, 70, 60, and 50%[a]

			CCSD(T)	$CCSD(T)_2^{OVOS}$			
Basis set	SCF	MP2	100%	80%	70%	60%	50%
cc-pVDZ	6.07	3.10	3.30	3.24	3.10	2.85	3.16
cc-pVTZ	6.07	2.32	2.65	2.64	2.58	2.61	2.66
cc-pVQZ	6.06	1.97	2.33	2.26	2.27	2.29	2.24
aug-cc-pVDZ	6.07	2.25	2.51	2.52	2.53	2.53	2.52
aug-cc-pVTZ	6.05	1.88	2.20	2.20	2.20	2.19	2.19
aug-cc-pVQZ	6.04	1.75	–	–	–	2.08	–
TZ→QZ [b]	–	–	–	–	–	2.00	–
aug-cc-pVDZ [c]	6.07	2.25	2.51	–	–	–	–

[a] BSSE-corrected[38] interaction energies in kcal/mol. 1s orbitals of C are frozen. [b] CCSD(T) CBS extrapolation (aug-cc-pVTZ → aug-cc-pVQZ). [c] Pittner and Hobza.[16]

where deformation of subsystems (A and B) is taken into account by a contribution defined as

$$\Delta E_{AB}^{AB} = [E_{AB}^{AB}(R_{AB}) - E_{A}^{AB}(R_{AB}) - E_{B}^{AB}(R_{AB})] + [E_{A}^{A}(R_{AB}) - E_{A}^{A}(R_{A})] + [E_{B}^{B}(R_{AB}) - E_{B}^{B}(R_{B})] \quad (7)$$

The notation is analogous to that in eq 6; i.e., subscripts represent a molecule and superscripts represent the supersystem (AB) or the subsystem (A or B) basis set. R_{AB} represents the optimized supersystem geometry, and R_A and R_B are the subsystem geometries, respectively.

Data in Table 3 demonstrate that the OVOS method performs excellently in considering the geometry relaxation terms. $\Delta E_{CCSD(T)_2}^{OVOS}$ interaction energies (OVOS truncated to 60%) and the full VOS $\Delta E_{CCSD(T)}$ agree to within 0.01−0.08 kcal/mol. Our full VOS $\Delta E_{CCSD(T)}$ and $\Delta E_{CCSD(T)_2}^{OVOS}$ results with the aug-cc-pVQZ basis set are −14.43 and −14.42 kcal/mol, respectively. These values represent probably the largest basis set CCSD(T) calculations for this dimer published so far. The CBS limit is −14.68 kcal/mol using aug-cc-pVXZ basis set results (X = T and Q) and the linear extrapolation[45] with respect to $1/X^3$. This value is by 0.2 kcal/mol less negative than $\Delta E_{CCSD(T)}$ published by Frey and Leutwyler[18] for the most stable FA···FA dimer. Their result was obtained by the exponential extrapolation using aug-cc-pVDZ to aug-cc-pV5Z MP2 interaction energies with the ΔCCSD(T) correction (−0.1 kcal/mol) calculated with the aug-cc-pVTZ basis set. Along with different techniques for obtaining the final $\Delta E_{CCSD(T)}$ interaction energy, there is a slight difference of geometries that we took from ref 16

3c. Interaction Energies of Model Stacking Formamide−Formamide and Ethylene−Ethylene Dimers. Model examples used for testing the performance of the OVOS technique for stacking intermolecular interactions are the parallel FO···FO and ET···ET sandwich dimers (see Figure 2). The stacking interaction energies of both systems are considerably smaller than the H-bonded energies. Energies presented in Tables 4 and 5 were calculated at fixed interplanar separation, 3.3 Å, which is typical for biological systems. This is the same distance as was considered in ref 16. At this distance, the SCF contribution to ΔE of the FO···FO dimer is attractive and represents 85% of the total CCSD(T) interaction energy with the full VOS of the aug-cc-pVQZ basis set. Small cc-pVDZ and cc-pVTZ basis sets are not applicable in this case and serve only as a demonstration of the excellent performance of OVOS in representing the basis set effects, as is transparently seen in Figure 5. The smallest basis set useful in calculations of the interaction energies of the stacked structure of FO···FO is the aug-cc-pVDZ basis set. The full VOS interaction energy, $\Delta E_{CCSD(T)}$, still deviates from the CBS limit by 0.31 kcal/mol, i.e., by 12% of the total interaction energy. As with H-bonded systems, it is much better to use large basis sets with OVOS truncated down to 50% of the full VOS than to use smaller basis sets. The error due to such a truncation of OVOS with all augmented bases is lower than 0.02 kcal/mol. The computer time is reduced to 10% when compared to the full VOS computer time.

A stacked ethylene dimer with the D_{2h} geometry shown in Figure 2 is characterized by a repulsive SCF interaction energy, which is insensitive to the basis set quality, unlike the attractive electron correlation energy contribution. When the ethylene planes are separated by 3.3 Å, the total ΔE remains repulsive. The attractive CCSD(T) electron correlation contribution is quite large, −3.9 kcal/mol, and is represented by OVOS truncated to 50% excellently (to within 0.01 kcal/mol with augmented basis sets), as is seen from data in Table 5. In Figure 6, we show the basis set dependence of ΔE with the full VOS CCSD(T) energies

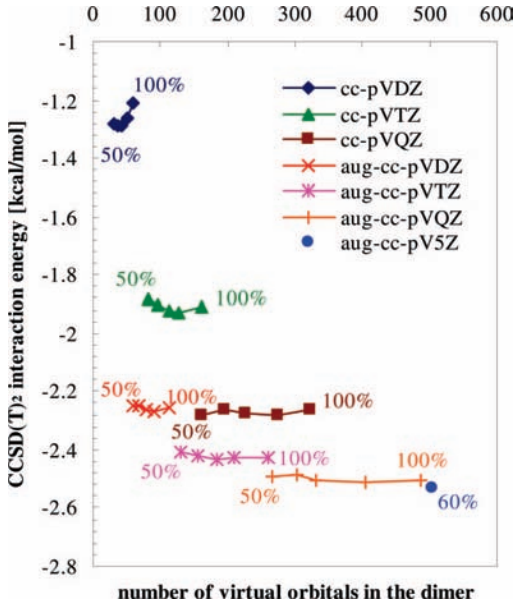

Figure 5. CCSD(T) interaction energies of the formaldehyde dimer (FO···FO; Figure 2) using cc-pVXZ (X = D, T, Q) and aug-cc-pVXZ (X = D, T, Q, 5) basis sets. 1s orbitals of C and O are frozen. Full VOS (100%) CCSD(T) and CCSD(T)$_2^{OVOS}$ interaction energies with OVOS truncated to 80−50%, respectively, are plotted as a function of the number of employed dimer virtual orbitals.

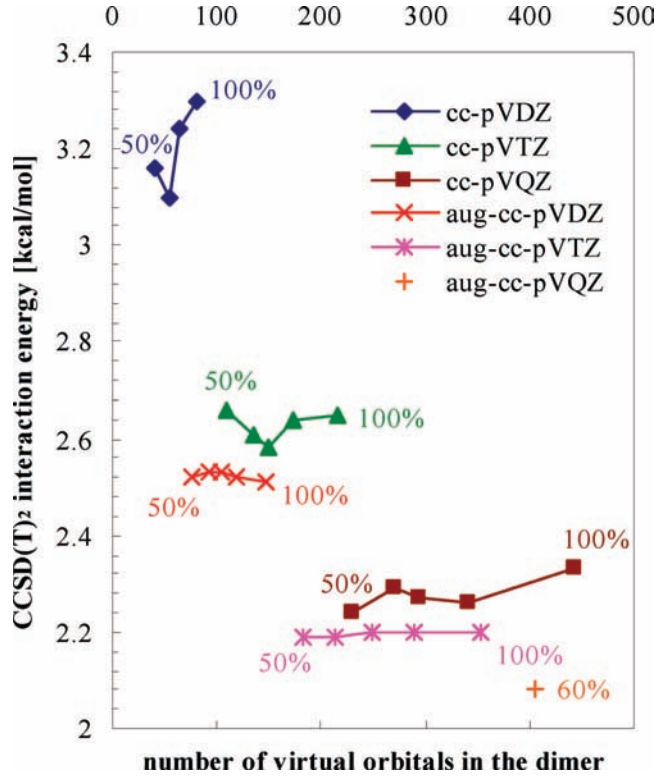

Figure 6. CCSD(T) interaction energies of the ethylene dimer (ET···ET; Figure 2) using cc-pVXZ (X = D, T, Q) and aug-cc-pVXZ (X = D, T, Q) basis sets. 1s orbitals of C are frozen. Full VOS (100%) CCSD(T) and CCSD(T)$_2^{OVOS}$ interaction energies with OVOS truncated to 80−50%, respectively, are plotted as a function of the number of employed dimer virtual orbitals.

and with OVOS reduced to 80, 70, 60, and 50%. The picture is essentially the same as that for the FO···FO stacking dimer (and, in fact, also for H-bonded dimers). We just note that when calculating the ethylene dimer in the high-symmetry D_{2h} structure, virtual orbitals distributed in eight symmetry representations must be truncated in OVOS considering the symmetry-equivalent orbitals.[14]

3d. Parallel Displacement in the Ethylene Dimer. Having verified the performance of OVOS in obtaining interaction energies of selected structures, we can use this method for other parts of the hypersurface for the displaced structure of the ethylene dimer. Although the absolute minimum of the ethylene dimer corresponds to the T-shaped structure,[31] parallel structures were more interesting as a model for stacking interactions in biological systems.

First, we point out that the D_{2h} sandwich structure represents actually a transition state between the two minima of slipped ethylene molecules. One example we report in Figure 7, with a fixed distance between the two ethylene planes, R_2 = 4.6 Å. The CCSD(T) energy with the full VOS and with OVOS truncated to 50% (the computational effort is reduced by about 1 order of magnitude) is varied with respect to the displacement distance, R_1. It is clear that with aug-cc-pVTZ and aug-cc-pVDZ basis sets OVOS performs excellently. OVOS truncated to 50% is even able to reproduce the deteriorated shape of the potential energy curve around the maximum (R_1 = 0) with the aug-cc-pVDZ basis set. Simply, this basis set is too small to be able to represent week interactions in the stacked ethylene dimer. With the larger aug-cc-pVTZ basis set, the barrier height at the curve (Figure 7) is 0.134 and 0.132 kcal/mol using the full VOS and OVOS truncated to 50%, respectively. With the aug-cc-pVDZ basis set, the barrier is by 0.02 kcal/mol higher and, again, well represented by OVOS. For the chosen R_2 = 4.6 Å distance, the dimer is slightly attractive due to dispersion forces. The minimum at the curve, of course, is far from the absolute energy minimum for the parallel displacement of the ET···ET dimer. For R_2 = 4.6 Å and R_1 = 0.0 Å, our sandwich structure of the

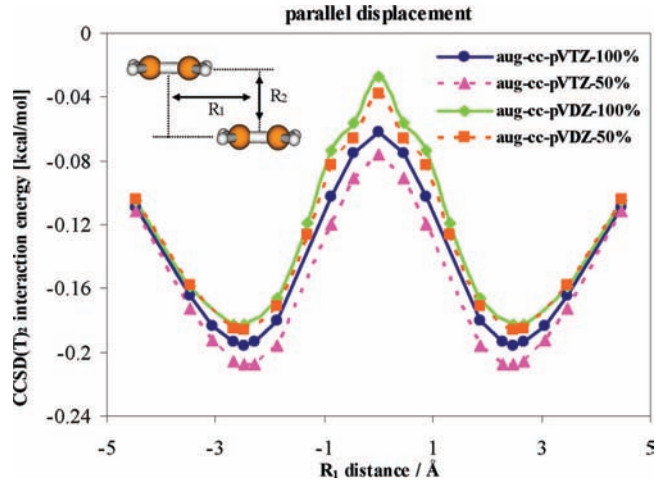

Figure 7. CCSD(T)$_2$ interaction energies [kcal/mol] of the stacked ethylene dimer with full VOS (100%) and OVOS reduced to 50% with aug-cc-pVXZ (X = D, T). The R_2 distance is fixed at 4.6 Å.

ethylene dimer is slightly more stable (−0.122 kcal/mol with the aug-cc-pVTZ basis set) than that from analogous MP2 results by Jalkanen et al.,[31] who used the 6-311+G(2df,2pd) basis set.

Optimization of the parallel slipping and stacking displacements R_1 and R_2, respectively, is shown in Figure 8 using the aug-cc-pVTZ basis set. Again, OVOS performs excellently. The minimum CCSD(T) energy is calculated at R_1 = 3.301 Å and R_2 = 3.040 Å, respectively, with the full VOS. With OVOS truncated to 50%, optimized distances are practically the same, R_1 = 3.299 Å and R_2 = 3.044 Å. Interaction energies with the full VOS and OVOS are −0.71 and −0.73 kcal/mol, respec-

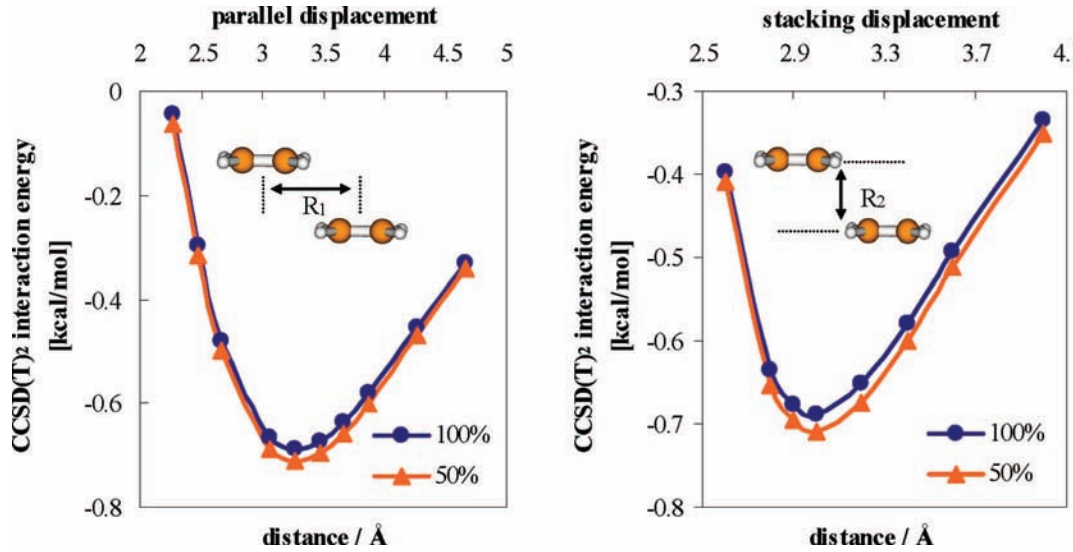

Figure 8. $CCSD(T)_2$ interaction energies [kcal/mol] of the stacked ethylene dimer with the full VOS (100%) and OVOS truncated to 50%. The aug-cc-pVTZ basis set. The parallel slipping curve was calculated at a fixed distance, $R_2 = 3.0$ Å, and the stacking displacement curve was calculated at fixed $R_1 = 3.3$ Å.

tively. MP2 overestimates the interaction energy (−0.83 kcal/mol) by 17%. For $R_2 = 3.04$ Å and $R_1 = 0.0$ Å (sandwich D_{2h} structure of the dimer), the energy is repulsive. We do not present this part of the curve in Figure 8.

4. Conclusions

Results for typical H-bonded formamide and formamidine dimers as well as for stacked formaldehyde and the ethylene dimers demonstrate the applicability of the OVOS technique in H-bonding and van der Waals interactions using the CCSD(T) method.

Nonaugmented cc-pVDZ and cc-pVTZ basis sets in calculations of H-bonded and particularly van der Waals dimers should be avoided. We recommend, instead, using larger basis sets, at least aug-cc-pVTZ with OVOS truncated to 60 or 50%. Errors introduced by truncating the VOS to 60% or even to 50% are much smaller than those due to using limited basis sets. At the same time, computational demands are reduced by about a factor of 6 or by about 1 order of magnitude (with OVOS truncated to 60% or 50%, respectively).

Our results show that using OVOS truncated to 60% or even to 50% of the full VOS can provide interaction energies of both H-bonded systems with an accuracy better than 0.02−0.1 kcal/mol. The basis set dependence of the full VOS CCSD(T) interaction energies is by 1 or 2 orders of magnitude larger.

Full VOS CCSD(T) interaction energies for stacked FO···FO and ET···ET systems with aug-cc-pVDZ and aug-cc-pVTZ basis sets differ typically by 0.2−0.3 kcal/mol, i.e., much more than that due to the truncation of OVOS to 60 or 50% (the deviation being typically 0.01 kcal/mol with doubly augmented basis sets).

The OVOS truncated to 50% performs excellently for calculations of the BSSE for fixed as well as for relaxed geometries of subsystems. It is essential that the percentage of the optimization functional L (eq 1) for a truncated OVOS with respect to the full VOS is the same for the supersystem and the subsystems.

Taking advantage of using OVOS truncated to 60%, we were able to calculate the CCSD(T) interaction energy in the H-bonded formamide dimer with the aug-cc-pV5Z basis set, which contains 1218 contracted Gaussian basis functions, using a dual processor AMD Opteron workstation. Our benchmark CBS limit for the interaction energy of this system is −16.34 kcal/mol. The geometry relaxation of the subsystems reduces this interaction energy by 1.62 kcal/mol (when the aug-cc-pVQZ basis set is used for this term). Our final $\Delta E^{OVOS}_{CCSD(T)_2}$ is −14.72 kcal/mol and appears to be the most accurate value of ΔE for this H-bonded dimer.

We have optimized the stacking and parallel displacement coordinates for the ethylene dimer. OVOS truncated to 50% reproduces the full VOS CCSD(T) results to within 0.004 Å. The barrier height, which separates the optimum stacked structures of the ET···ET dimer from its sandwich D_{2h} transition structure (0.134 kcal/mol with the full VOS with the aug-cc-pVTZ basis set) is reproduced by OVOS to within 0.002 kcal/mol.

The OVOS technique, when combined with sophisticated programming and high-level parallelism, opens a route for CCSD(T) calculations of larger H-bonded or stacked dimers. This may lead to reliable calculations of interaction energies of more realistic biologically important model systems, like the uracil dimer.[15] Closely related is the method employing frozen natural orbitals.[46] We believe that OVOS may serve as a general alternative to other methods,[47–55] such as local electron correlation methods[47–49,51,52] or symmetry-adapted perturbation theory (SAPT) methods.[53–55] We note that the OVOS method may be useful also in other areas of computational chemistry as a tool for accurate predictions of molecular properties.[14]

Acknowledgment. The support of the Slovak Research and Development Agency (Contract APVV-20-018405) and VEGA (Grant 1/3560/06) is gratefully acknowledged. P.D. is thankful for a grant awarded by Comenius University to young scientists.

References and Notes

(1) Jurečka, P.; Černý, J.; Hobza, P.; Salahub, D. R. *J. Comput. Chem.* **2007**, *28*, 555.
(2) Zhao, Y.; Truhlar, D. G. *Chem. Phys. Phys. Chem.* **2005**, *7*, 2701.
(3) Jurečka, P.; Šponer, J.; Černý, J.; Hobza, P. *Phys. Chem. Chem. Phys.* **2006**, *8*, 1985.
(4) Raghavachari, K.; Trucks, G. W.; Pople, J. A.; Head-Gordon, M. *Chem. Phys. Lett.* **1989**, *157*, 479.
(5) Urban, M.; Noga, J.; Cole, S. J.; Bartlett, R. J. *J. Chem. Phys.* **1985**, *83*, 4041.

(6) Urban, M.; Černušák, I.; Kellö, V.; Noga, J. In *Methods in Computational Chemistry*; WilsonS. E., Ed.; Plenum Press: New York, 1987; Vol. 1, p 117.

(7) Janowski, T.; Ford, A. R.; Pulay, P. *J. Chem. Theor. Comput.* **2007**, *3*, 1368.

(8) Neogrády, P.; Aquilante, F.; Noga, J.; Pitoňák, M.; Urban, M., in preparation, 2008.

(9) Adamowicz, L.; Bartlett, R. J. *J. Chem. Phys.* **1987**, *86*, 6314.

(10) Adamowicz, L.; Bartlett, R. J.; Sadlej, A. J. *J. Chem. Phys.* **1988**, *88*, 5749.

(11) Neogrády, P.; Pitoňák, M.; Urban, M. *Mol. Phys.* **2005**, *103*, 2141.

(12) Pitoňák, M.; Holka, F.; Neogrády, P.; Urban, M. *THEOCHEM* **2006**, *768*, 79.

(13) Pitoňák, M.; Neogrády, P.; Kellö, V.; Urban, M. *Mol. Phys.* **2006**, *104*, 2277.

(14) Urban, M.; Pitoňák, M.; Neogrády, P. Optimized virtual orbital space (OVOS) as a tool for more efficient correlated and relativistic calculations of molecular properties and interactions. In *Lecture Series on Computer and Computational Science*; Maroulis, G., Simos, T., Eds.; Brill Academic Publishers: Leiden, 2006; Vol. 6, p 265.

(15) Pitoňák, M.; Riley, K. E.; Neogrády, P.; Hobza, P. *Chem.—Eur. J.* **2008**, in press, DOI: 10.1002/cphc.200800286.

(16) Pittner, J.; Hobza, P. *Chem. Phys. Lett.* **2004**, *390*, 496.

(17) Mardyukov, A.; Sanchez-Garcia, E.; Rodziewicz, P.; Doltsinis, N. L.; Sander, W. *J. Phys. Chem. A* **2007**, *111*, 10552.

(18) Frey, J. A.; Leutwyler, S. *J. Phys. Chem. A* **2006**, *110*, 12512.

(19) Vargas, R.; Garza, J.; Friesner, R. A.; Stern, H.; Hay, B. P.; Dixon, D. A. *J. Phys. Chem. A* **2001**, *105*, 4963.

(20) Marigliano, A. C. G.; Varetti, E. L. *J. Phys. Chem. A* **2002**, *106*, 1100.

(21) Jurečka, P.; Hobza, P. *Chem. Phys. Lett.* **2002**, *365*, 89.

(22) Šponer, J.; Hobza, P. *J. Phys. Chem. A* **2000**, *104*, 4592.

(23) Gora, R. W.; Grabowski, S. J.; Leszczynski, J. *J. Phys. Chem. A* **2005**, *109*, 6397.

(24) Lim, J. H.; Lee, E. K.; Kim, Y. *J. Phys. Chem. A* **1997**, *101*, 2233.

(25) Kemper, M. J. H.; Hoeks, C. H.; Buck, H. M. *J. Chem. Phys.* **1981**, *74*, 5744.

(26) Ford, T. A.; Glasser, L. *THEOCHEM* **1997**, *398*, 381.

(27) Hermida-Ramon, J. M.; Rios, M. A. *J. Phys. Chem. A* **1998**, *102*, 10818.

(28) Tsuzuki, S.; Uchimaru, T.; Mikami, M.; Tanabe, K. *Chem. Phys. Lett.* **1996**, *252*, 206.

(29) Curutchet, C.; Cammi, R.; Mennucci, B.; Corni, S. *J. Chem. Phys.* **2006**, 125.

(30) Chan, M. C.; Block, P. A.; Miller, R. E. *J. Chem. Phys.* **1995**, *102*, 3993.

(31) Jalkanen, J. P.; Pulkkinen, S.; Pakkanen, T. A.; Rowley, R. L. *J. Phys. Chem. A* **2005**, *109*, 2866.

(32) Lovas, F. J.; Suenram, R. D.; Coudert, L. H.; Blake, T. A.; Grant, K. J.; Novick, S. E. *J. Chem. Phys.* **1990**, *92*, 891.

(33) Vila, A.; Grana, A. M.; Mosquera, R. A. *Chem. Phys.* **2002**, *281*, 11.

(34) Karlstrom, G.; Lindh, R.; Malmqvist, P. A.; Roos, B. O.; Ryde, U.; Veryazov, V.; Widmark, P. O.; Cossi, M.; Schimmelpfennig, B.; Neogrády, P.; Seijo, L. *Comput. Mater. Sci.* **2003**, *28*, 222.

(35) Neogrády, P.; Pitoňák, M.; Urban, M. *Mol. Phys.* **2005**, *103*, 2141.

(36) Dunning, T. H. *J. Chem. Phys.* **1989**, *90*, 1007.

(37) Kendall, R. A.; Dunning, T. H.; Harrison, R. J. *J. Chem. Phys.* **1992**, *96*, 6796.

(38) Boys, S. F.; Bernardi, F. *Mol. Phys.* **1970**, *19*, 553.

(39) Frisch, M. J.; Trucks, G. W.; Schlegel, H. B.; Scuseria, G. E.; Robb, M. A.; Cheeseman, J. R.; Montgomery, J. J. A.; Vreven, T.; Kudin, K. N.; Burant, J. C.; Millam, J. M.; Iyengar, S. S.; Tomasi, J.; Barone, V.; Mennucci, B.; Cossi, M.; Scalmani, G.; Rega, N.; Petersson, G. A.; Nakatsuji, H.; Hada, M.; Ehara, M.; Toyota, K.; Fukuda, R.; Hasegawa, J.; Ishida, M.; Nakajima, T.; Honda, Y.; Kitao, O.; Nakai, H.; Klene, M.; Li, X.; Knox, J. E.; Hratchian, H. P.; Cross, J. B.; Bakken, V.; Adamo, C.; Jaramillo, J.; Gomperts, R.; Stratmann, R. E.; Yazyev, O.; Austin, A. J.; Cammi, R.; Pomelli, C.; Ochterski, J. W.; Ayala, P. Y.; Morokuma, K.; Voth, G. A.; Salvador, P.; Dannenberg, J. J.; Zakrzewski, V. G.; Dapprich, S.; Daniels, A. D.; Strain, M. C.; Farkas, O.; Malick, D. K.; Rabuck, A. D.; Raghavachari, K.; Foresman, J. B.; Ortiz, J. V.; Cui, Q.; Baboul, A. G.; Clifford, S.; Cioslowski, J.; Stefanov, B. B.; Liu, G.; Liashenko, A.; Piskorz, P.; Komaromi, I.; Martin, R. L.; Fox, D. J.; Keith, T.; Al-Laham, M. A.; Peng, C. Y.; Nanayakkara, A.; Challacombe, M.; Gill, P. M. W.; Johnson, B.; Chen, W.; Wong, M. W.; Gonzalez, C.; Pople, J. A. *Gaussian 03*; Gaussian, Inc.: Wallingford, CT, 2004.

(40) Moller, C.; Plesset, M. S. *Phys. Rev.* **1934**, *46*, 618.

(41) Neogrády, P.; Medved, M.; Černušák, I.; Urban, M. *Mol. Phys.* **2002**, *100*, 541.

(42) Šulka, M.; Pitoňák, M.; Neogrády, P.; Urban, M. *Int. J. Quantum Chem.* **2008**, *108*, 2159.

(43) Tzeli, D.; Mavridis, A.; Xantheas, S. S. *J. Phys. Chem. A* **2002**, *106*, 11327.

(44) Šimová, L.; Tzeli, D.; Urban, M.; Černušák, I.; Theodorakopoulos, G.; Petsalakis, I. D. *Chem. Phys.* **2008**, in press (online March 4, 2008).

(45) Halkier, A.; Helgaker, T.; Jorgensen, P.; Klopper, W.; Koch, H.; Olsen, J.; Wilson, A. K. *Chem. Phys. Lett.* **1998**, *286*, 243.

(46) Taube, A. G.; Bartlett, R. J. *Collect. Czech. Chem. Commun.* **2005**, *70*, 837.

(47) Boughton, J. W.; Pulay, P. *J. Comput. Chem.* **1993**, *14*, 736.

(48) Korona, T.; Pfluger, K.; Werner, H. J. *Phys. Chem. Chem. Phys.* **2004**, *6*, 2059.

(49) Hill, J. G.; Platts, J. A.; Werner, H. J. *Phys. Chem. Chem. Phys.* **2006**, *8*, 4072.

(50) Bludský, O.; Rubeš, M.; Soldán, P.; Nachtigall, P. *J. Chem. Phys.* **2008**, *128*, 114102.

(51) Friedrich, J.; Hanrath, M.; Dolg, M. *J. Phys. Chem. A* **2007**, *111*, 9830.

(52) Maslen, P. E.; Dutoi, A. D.; Lee, M. S.; Shao, Y. H.; Head-Gordon, M. *Mol. Phys.* **2005**, *103*, 425.

(53) Jeziorski, B.; Moszynski, R.; Szalewicz, K. *Chem. Rev.* **1994**, *94*, 1887.

(54) Korona, T.; Jeziorski, B. *J. Chem. Phys.* **2008**, *128*, 144107.

(55) Podeszwa, R.; Bukowski, R.; Szalewicz, K. *J. Phys. Chem. A* **2006**, *110*, 10345.

JP8033903